Morphology of Latex Particles Formed by Poly(methyl Methacrylate)-Seeded Emulsion Polymerization of Styrene

IWHAN CHO and KYUNG-WOO LEE, *Department of Chemistry, Korea Advanced Institute of Science and Technology, P.O. Box 150 Chongyangni, Seoul 131, Korea.*

Synopsis

Poly(methyl methacrylate)–polystyrene composite particle latexes were prepared by poly(methyl methacrylate)-seeded emulsion polymerization of styrene employing batch, swelling-batch, and semibatch methods. The changes in particle morphology taking place during the polymerization reaction were followed by electron microscopy. Anchoring effect exerted by ionic terminal groups introduced by ionic initiator was found to be the main factor in controlling the particle morphology. The polymer particles obtained by oil-soluble hydrophobic initiators such as azobisisobutyronitrile and 4,4'-azobis-(4-cyanovaleric acid) gave the inverted core-shell morphology. Water-soluble hydrophilic initiator, $K_2S_2O_8$, also gave the inverted core-shell morphology. However, in this case the occurrence of the halfmoonlike, the sandwichlike, and the core-shell morphologies were also observed depending upon the polymerization conditions. The distribution of terminal $-SO_4^-$ groups on the surface area of polystyrene particles could be controlled by initiator concentration and polymerization temperature. Viscosity of polymerization loci dictated the movement of polymer molecules, thus causing the unevenness of particle shape and phase separation at high viscosity state. Viscosity was controlled by the styrene/poly(methyl methacrylate) ratio, the addition of a chain transfer agent or a solvent which is common to polystyrene and poly(methyl methacrylate).

INTRODUCTION

Control of latex particle morphology is important for many practical applications.[1] Latex particles of different morphological features have been prepared from seeded emulsion polymerization techniques. This technique has been employed for various kinetic[2] and morphology studies involving homo- and heterogeneous polymer pair systems.

Hughes and Brown[3] were the first to investigate the physical properties of heterogeneous composite polymer particles, and Paxton[4] followed and confirmed the results employing the polystyrene (PS)-core/poly(methyl methacrylate) (PMMA)-shell system with soap titration method. Dickie and his co-workers[5] studied the particle morphology of heterogeneous acrylic latex particles (a pair of glassy and rubbery polymers) by transmission electron microscopy and minimum film-forming temperature method. In a series of works Okubo and his co-workers[6–11] showed that heterogeneous composite polymer particles could change its particle morphology from confettilike to raspberrylike and/or void-containing, depending upon the molecular weights of polymers, viscosity of polymerization loci, polymerization condition, and the difference in hydrophilicity of two polymers. Lee and his co-worker[12–14] studied the effects of stage ratio, molecular weights of poly-

Journal of Applied Polymer Science, Vol. 30, 1903–1926 (1985)
 CCC 0021-8995/85/051903-24$04.00

mers, and the hydrophilicity of polymers on the particle morphology and summarized well the various types in the particle morphology. Recently, Min and his co-workers[15] have shown that the morphology of poly(butyl acrylate) (PBA)–PS composite latex particle was affected by the adhesion effect exhibited by the byproduct graft copolymer distributed at the interface of two different polymers in a particle.

Selective staining of double bonds in polymer backbones by OsO_4[16] makes transmission electron microscopy a useful tool for the morphological study of polymer blends. Recently, Trent and his co-workers[17] have found that RuO_4 could stain PS region selectively in PS–PMMA blends. They also reported that RuO_4 could stain certain other polymers which were not stained by OsO_4.

Most of the works reported hitherto are limited to the morphology and the physical properties of glassy–rubbery polymer pair systems,[3,5–8,11–13,18] the reason being that the prepared composite polymers might have certain improved properties. Lacking in the literatures are the studies on the change of the particle morphology which are taking place particularly during the polymerization reactions. In the present work we have taken a glassy–glassy polymer pair system (PS–PMMA) and followed the change of latex particle morphology. Various polymerization parameters were taken into account, and the change of the particle morphology during the polymerization reaction was monitored by taking transmission electron micrographs (TEMs) with RuO_4-staining method and scanning electron micrographs (SEMs). For the clearer interpretation the monodispersed PMMA seed latexes were used.

EXPERIMENTAL

Materials. Reagent grade styrene and methyl methacrylate (MMA) were distilled under reduced pressure. The middle fraction was cut and stored in a refrigerator. Sodium dodecylbenzene sulfonate (SDBS, Siponate DS-10 from Alcolac Chemical Co.), and Triton X-100 (polyoxyethylene isooctylphenylether from Rohm and Haas Co.) were used without further purification. Water was redistilled from basic $KMnO_4$ solution. Other chemicals were analytical grade reagents and used without further purification.

Polymerization. All the polymerizations were performed in 1-L flasks under N_2 purging. Each flask was equipped with a paddle-type stirrer, a reflux condenser, a sampling tube, a dropping funnel, and thermocouples. Polymerization temperature was controlled by electrically regulated heating mantle and recorded with Linear 141 recorder. Agitation speeds were 120 rpm for MMA polymerization and 200 rpm for PMMA-seeded styrene polymerization. N_2 purging was started with the charge of ingredients into the flask and continued to the peak time. In a general procedure all the ingredients were first charged and then the system was heated to the required temperature before the addition of initiator solution. Because of the large heat of polymerization the temperatures of PMMA polymerization could not be controlled rigorously. After the peak time the reaction systems were heat-treated at 95°C for 2 h and then cooled with an ice-water bath to ambient temperature.

In semibatch polymerizations, the monomer was added dropwise to the preheated reaction mixture, the addition rate being kept at 0.6 mL/min. To follow the conversions and the morphological change of latex particles taking place during the polymerization process, aliquots of the latex (20–30 mL) were taken out at certain time intervals and hydroquinone solution was added to stop the polymerization. Total solid contents (TSCs) were determined gravimetrically.

Particle Morphology. The morphology of latex particles were studied by three kinds of electron microscopic methods; latex TEMs, latex SEMs, and RuO_4-stained thin section TEMs. General procedures for electron microscopic work are as follows:

(1) The apparent cross-sectional shapes of latex particles were observed by latex TEMs. A latex sample diluted (ca. 50 ppm) with water was dropped on the collodion-coated copper grid and then dried in open air. The residual monomer and other volatile matters were removed under vacuum before the micrographs were taken.

(2) For SEMs the dried latex grids prepared as above were placed in an ion sputter (JFM-1000) and then coated with Au. The coating thickness was about 50 Å. The 3-dimensional shapes of particles were then observed from those specimens with SEM mode, and the desired photographs were taken.

(3) The internal morphology of latex particles was determined as follows: The latex (TSC, ca. 10%) which had been dialyzed usually for more than 7 days using a Visking cellophane tube was spread on a clean slide glass and dried in air. Because of the high glass transition temperature (PS, 100°C; PMMA, 105°C), the particles did not form film but small flat fragments. The fragments were dried overnight at 60°C in a vacuum oven and then transferred into BEEM capsules carefully, Epon 812 epoxy resin was used for embedding and cured at 60°C for 18 h. The cured blocks were sectioned with LKB Ultratome V ultramicrotome (thickness, ca. 900 Å). These thin sections were mounted on copper grids, dried in air, and stained over 0.1% aqueous RuO_4 solution for 12 h. The stained sample grids were dried under vacuum overnight before taking electron micrographs.

(4) Shadow casting: Being different from PS particles the PMMA particles were shrunk by electron beam during the process, of taking TEMs. Therefore, for the determination of precise particle size, the dried PMMA latex grids, prepared as above [(1)], were shadowed with silver metal in Vacuum Evaporater (JEM-4X, manufactured by JEOL Co.). In a common procedure the sizes of 100–300 particles were measured, and the values averaged.

The weight average D_w, and the number average D_n diameters and the dispersity U of PMMA latex particles were calculated as follows:

$$D_w = \left(\sum n_i D_i^6 / \sum n_i D_i^3\right)^{1/3}$$

$$D_n = \left(\sum n_i D_i / \sum n_i\right)$$

$$U = D_w / D_n$$

where n_i is the number of particles in the latex having diameter D_i. A

standard PS latex (D_n = 2538 Å, standard deviation = 31 Å), supplied by Dow Chemical Co. through the courtesy of Dr. D. I. Lee, was used as an internal standard for size calibration.

TEMs and SEMs of these samples were obtained with a JEOL 100-CX Electron Microscope. Accelerating voltages of electron beam were 60–100 kV for TEMs and 20 kV for SEMs.

Intrinsic Viscosity. Latexes were coagulated with hot acidic methanol (1 vol % concn H_2SO_4/CH_3OH). The precipitates were filtered and then washed with a large volume of water. Thus obtained solid polymers were reprecipitated with THF–methanol and dried in a vacuum oven at 60°C to constant weight. Intrinsic viscosities of PMMAs were determined at 30 ± 0.1°C with a Cannon-Fenske No. 50 Viscometer (concn, 0.5 g/dL; solvent, toluene) and calculated by the one-point method.

Swelling of Latex Particles. The swelling rates and the equilibrium swelling ratio of PMMA latexes with styrene were measured under the similar conditions employed for the polymerizations. Aliquots of collected latex samples during the swelling experiments were centrifuged at 3000 rpm for 5 min. Then the styrene-swollen latexes were withdrawn by a hypodermic syringe, and TSC was measured gravimetrically. Those TSC values at 60°C and 80°C for the latex samples were quenched with an ice-water bath and then the same procedures were applied. The swelling ratio was calculated from TSCs before and after the swelling.

Other Measurements. Surface tension and interfacial tension were measured at room temperature by du Nouy ring methods. pH values of latexes were determined by pH meter at room temperature after the heat treatment.

RESULTS AND DISCUSSION

Preparation of Seed PMMA Latexes

Polymerization conditions and the properties of the resulting PMMA latexes are summarized in Table I. Because of the difficulty in the control of the polymerization temperature, the particle size of the resulting latexes did not turn out as expected, even when the similar polymerization conditions were employed. The easy radical desorption caused by chain transfer agents decreased the particle size, exhibiting little effect on the molecular weights. The high surface tension of PMMA latexes showed that the surface of PMMA latex particles were not completely covered with emulsifiers. At any event, as shown in Table I, the particle size distribution of each PMMA latex obtained in the present study showed good monodispersity.

Seeded Emulsion Polymerization

Emulsion polymerization takes place in complicated mechanisms, and the rate of polymerization and the morphology of latex particles can be affected by many reaction parameters. In the present study the particle nucleation stage of emulsion polymerization was bypassed by employing seeding technique and new particle nucleation was minimized. In some cases

TABLE I
Polymerization Conditions and Properties of Seed Poly(methyl Methacrylate) Latexes

Sample name	PMMA-1	PMMA-2	PMMA-3	PMMA-4	PMMA-5	PMMA-6	PMMA-7
Ingredients[a]							
H_2O	180	180	180	180	180	180	180
MMA	100	100	100	100	100	100	100
Triton X-100	3.01	3.0	3.0	3.0	3.0	3.0	3.0
SDBS	0.30	0.30	0.30	0.15	0.30	0.30	0.15
$K_2S_2O_8$	0.5	0.5	0.49	0.5	0.5	0.5	0.5
$CHBr_3$	0	0	0	0	0.5	2.3	0
Properties							
D_n (Å)	1560	1610	1700	3180	1330	1170	2570
U	1.003	1.003	1.002	1.001	1.002	1.004	1.001
pH	2.15	2.20	2.90	2.35	2.40	2.50	2.95
Surface tension (dyn/cm)	44.5	46.4	45.3	42.3	48.9	50.6	43.6
Intrinsic viscosity	1.78	1.75	1.74	1.82	1.74	1.60	2.11

[a] Quantities are in weight parts.

the new particle nucleation was observed, but its amount was too small to affect the system.

Swelling Time

Smith and Ewart[19] assumed that during the emulsion polymerization the monomer concentration in polymerizing particles was independent of conversion as long as monomer droplets were present in the system. Morton and his co-workers[20] reported the fast diffusion rate of toluene into PS latex particles. In those cases the latex particles were small ($D_n \leq 1000$ Å). However, Chung-Li and his co-workers[21] showed that when larger seed particles were used, the diffusion of monomer into the seed PS particles could be a slow process.

Matsumoto and his co-workers[6] claimed that the particle morphology was affected by the swelling state. Min and his co-workers[15] reported that the swelling state affected the formation of grafted copolymers and the long-term morphology change of PBA–PS composite latex particles.

In the present study we made an attempt to follow closely the effects of swelling state on the particle morphology. As shown in Table II, PMS-5 and -6 showed the same rate of polymerization in spite of the difference in the swelling time. And in Figure 1 the two latex particles appeared as the

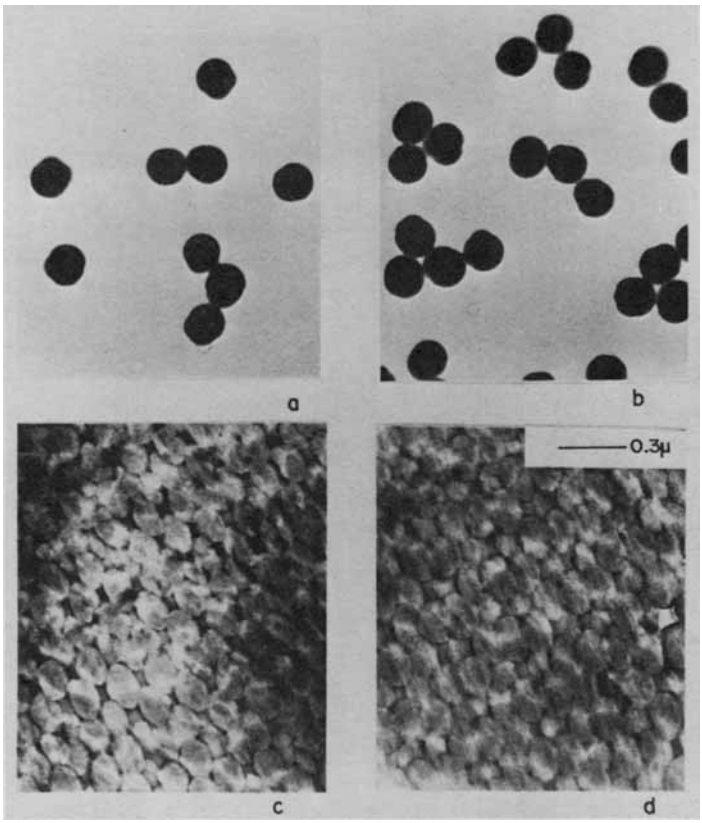

Fig. 1. Effect of swelling time on the particle morphology. (a) and (b) are latex TEMs and (c) and (d) are TEMs of RuO_4-stained thin sections. PMS-5 [(a) and (c); swelling time, 1 h] and PMS-6 [(b) and (d) swelling time, 4 days]. In (c) and (d) the dark part in a particle is the PS-rich region and the bright part is the PMMA-rich region.

TABLE II
Polymerization Conditions and Results of PMMA-Seeded Emulsion Polymerization of Styrene at 60°C[a]

Experimental no.	PMS-5	PMS-6	PMS-13	PMS-16	PMS-12
Ingredients					
Water	100	100	100	97.5	95
PMMA (species)[b]	5 (-1)	5 (-1)	5 (-2)	5 (-2)	5 (-2)
Styrene	15	15	15	15	15
$K_2S_2O_8$	0.1	0.1	0.1	0.1	0.1
KOH (0.1*N*)	—	—	0.5	2.5	5
Conditions					
Swelling time (days)	—	4	—	—	—
pH	2.8	3.0	3.0	5.7	10.6
Rate of polymerization ($\times 10^2$ g/min)	3.75	3.87	3.63	3.47	3.50

[a] Quantities are in weight parts.
[b] Weight of seed latex is on dry base.

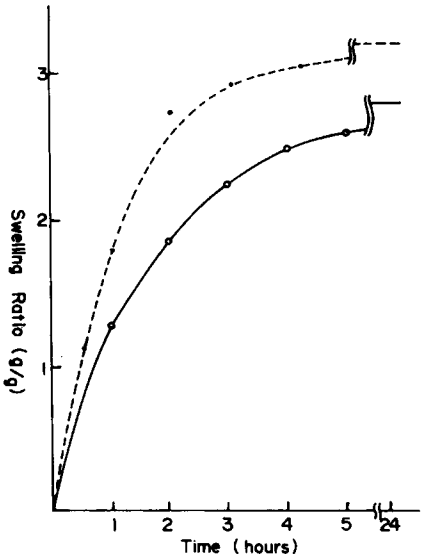

Fig. 2. Swelling rates of seed latexes, PMMA-1 (○) and -4 (●), by styrene at room temperature. Swelling ratio is the weight of styrene required to swell the unit weight of PMMA.

same "halfmoonlike" morphology. It was obvious from these results that the particle morphology and the rate of polymerization were not affected by the swelling time at least in the system presently investigated.

The swelling rates of PMMA latexes (PMMA-1 and -4) with styrene at room temperature are shown in Figure 2, and the equilibrium swelling ratios (the weight of swollen styrene/the weight of PMMA) of them are given in Table III. The equilibrium swelling ratio decreased with the increasing polymerization temperature and increased with the particle size. In our batch polymerization procedure the elapsing time starting from the ingredients charge to the initiator addition was about 1 h, and the swelling ratio of PMMA-1 (in PMS-5 polymerization) just before the initiator addition (at 60°C) was 1.76 g/g. Although the equilibrium swelling ratio of PMMA-1 at room temperature was 2.79 g/g, it decreased to 1.51 g/g at 60°C. Regardless of the length of the swelling time at room temperature, the swelling ratios at polymerization temperature were similar in all of our polymerization systems. Therefore, it can be stated that the particle morphology and the rate of polymerization were not affected by the swelling time.

TABLE III
Equilibrium Swelling Ratios of PMMA-1 and -4 at Various Temperatures[a]

	Room temp	60°C	80°C
PMMA-1	2.79	1.51	1.37
PMMA-4	3.20[b]	2.41	1.80

[a] Swelling Test Conditions: water, 95; PMMA (dry weight), 5; styrene, 16; hydroquinone, 0.1 (weight part)

[b] Maximum swelling ratio of this system, not equilibrium swelling ratio.

pH Effects

In the PS-seeded emulsion polymerizations of styrene[22] pH of the reaction system did not affect the polymerization, when the value was greater than 4.0. It has been known[23] that the rate of decomposition of $K_2S_2O_8$ remains almost unchanged through pH range between 3 and 12, but below 3 the rate increases sharply. In PMMA–styrene systems the rate of polymerization (Table II; PMS-13, -16, and -12) and the particle morphology were not affected by pH of the polymerization medium in this pH range, as expected.

Effects of Initiators

Three initiators, $K_2S_2O_8$, azobisisobutyronitrile (AIBN), and 4,4'-azobis-(4-cyanovaleric acid) (ABCVA), were used for the study. $K_2S_2O_8$-initiated polymerizations under different conditions are summarized in Table IV. The representative TEMs showing the change in apparent latex particle shape and morphology taking place during the polymerization under different reaction conditions are shown in Figures 3–5. The latex particles being in the polymerization process were swollen with styrene, but the particles became a monomer-free state when subjected to the procedures for TEM.

In a colloidal particle the external mixing of dispersing medium usually

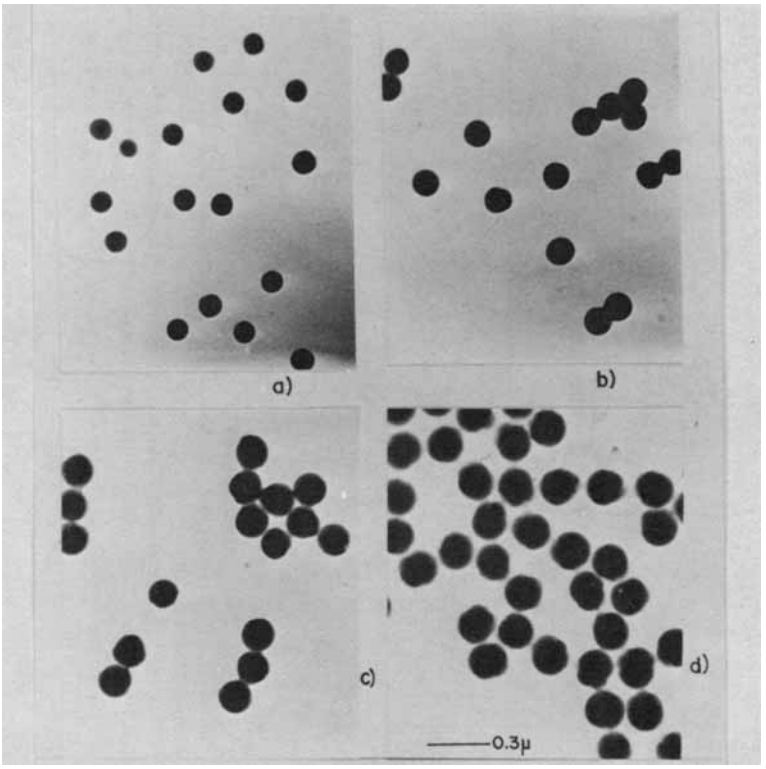

Fig. 3. Change in apparent latex shape during the polymerization of PMS-19 at 60°C. The monomer conversions were (a) 10.5%, (b) 21.3%, (c) 52.1%, and (d) 93.5%. The volume growth ratio (5.54/1) of particles between (a) and (d) is greater than the calculated value (3.43/1). It was caused by the volume shrinkage of PMMA latexes under the electron beam in electron microscope. Halfmoonlike morphology is clearly seen in (c).

TABLE IV
Effects of Different Initiators under Different Conditions upon Polymerizations

	PMS-19	-24	-30	-31	-49	-52	-54	-55
Ingredients								
Water	95	90	95	95	98	100	96	96
PMMA (species)	5 (-3)	5 (-3)	5 (-4)	5 (-4)	5 (-7)	5 (-7)	5 (-1)	5 (-4)
Styrene	15	15	15	15	15	15	15	15
KOH (0.1*N*)	5	10	5	5	2		4	4
AIBN					0.1			
ABCVA								0.1
$K_2S_2O_8$	0.1	0.1	0.1	0.1		0.4	0.003	
Conditions								
Polymerization temp (°C)	60	80	80	60	80	60	80	80

[a] Quantities are in weight parts.

[b] When AIBN was used, the final latex had larger amount of coagulum (ca. 2–4 parts), but the coagulum could be minimized (ca. 0.1 part) by sufficient premixing of AIBN with seed latex added with styrene solution (5 parts) at room temperature.

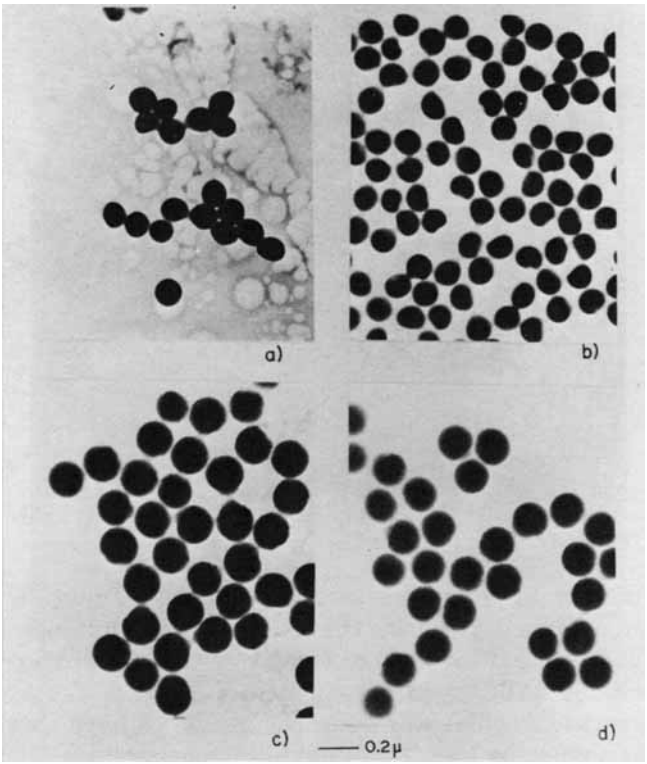

Fig. 4. Change in apparent latex shape during the polymerization of PMS-24 at 80°C. The monomer conversions were (a) 12.1%, (b) 30.0%, (c) 56.6%, and (d) 99.9%. The void-containing particles are seen in (b).

does not perturb the internal phase of the particle. Therefore, the polymerizing particles were in a quasistatic state, and the particle morphology was determined by the thermodynamic factors such as polymer incompatibility and interfacial tension. The kinetic factors such as mobility of polymer and viscosity of polymerization loci could also be operative.

Styrene was a common solvent to PS and to PMMA, but at high polymer concentration (the maximum weight fraction of styrene in these systems was 0.75) the PS– and PMMA–styrene phase started to separate[24,27] as soon as styrene polymerization took place. In such a process the graft copolymer was formed during the seeded polymerization[3,15] and distributed at the interfacial area of PS–PMMA, thus contributing to stabilize the separated domains in each particle.

Lee and Ishikawa[14] and Matsumoto et al.[6] showed that in the hydrophilic–hydrophobic polymer pair systems the morphology of particles depended upon hydrophilicity, stage ratio, molecular weight, viscosity, and polymerization methods. And when hydrophobic polymers were polymerized with hydrophilic polymer seeds it was shown that the second polymers were surrounded by seed polymer. This so-called "inverted core-shell" morphology caused by the higher hydrophilicity of seed PMMA was well observed also in our system, when oil-soluble (AIBN) or water-soluble but less hy-

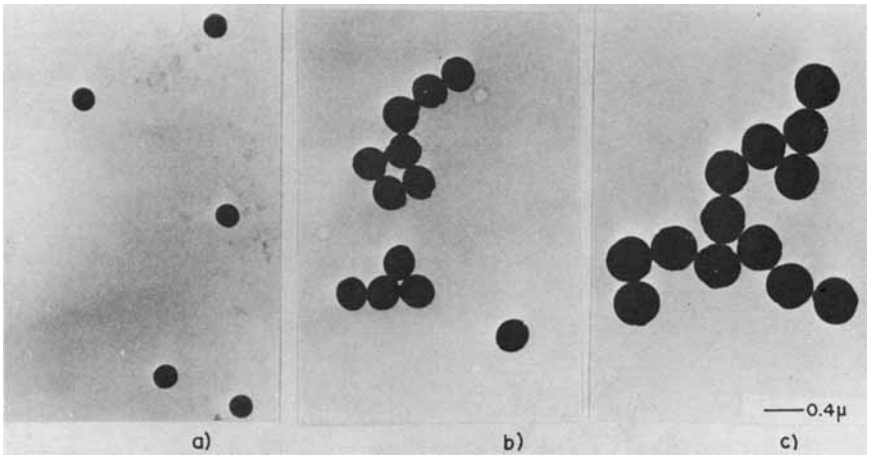

Fig. 5. Change in apparent latex shape during the polymerization of PMS-31 at 60°C. The monomer conversions were (a) 3.7%, (b) 31.4%, and (c) 92.5%. The sandwichlike particles are seen in (b).

drophilic (ABCVA) initiator were used. As shown in Figure 6, the hydrophobic PS-rich domain grew inside the relatively more hydrophilic PMMA-rich matrix and formed "inverted core-shell" morphology. The same trend was observed in the ABCVA-initiated polymerization.

In the contrast with what was described above we have obtained interesting results with ionic $K_2S_2O_8$-initiated polymerization systems. In this case the particle morphology was little affected by the difference in the hydrophilicity of PMMA and PS, but rather depended upon the initiator concentration and polymerization temperature. When the initiator concentration was low (PMS-54, concentration 0.003 g/dL), the PS-rich domain grew inside of the PMMA-rich matrix in a particle as illustrated in Figure 7. However, this formation of inverted core-shell morphology was not as clear as in the case of PMS-49. In case of PMS-31 (Fig. 8) the PS-rich domain grew first at the tips of PMMA particles, and gradually the PS-rich domains surrounded the PMMA-rich regions as the polymerization proceeded, thus the PMMA-rich region becoming sandwiched by PS-rich domains. We here-

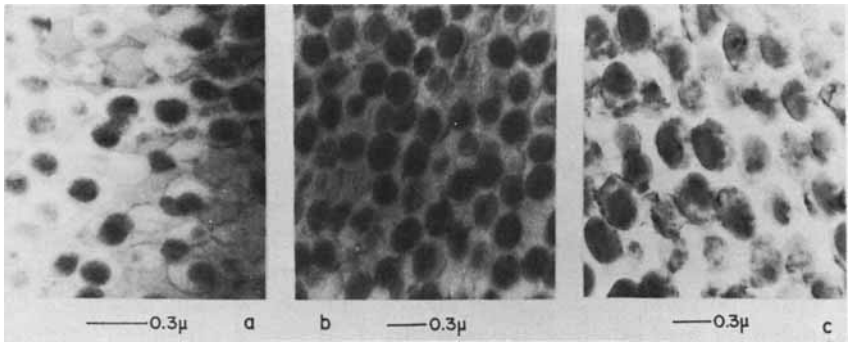

Fig. 6. TEMs of RuO_4-stained thin sections. Change in internal particle morphology of PMS-49 during the polymerization at 80°C with AIBN. The monomer conversions were (a) 9.1%, (b) 28.0%, and (c) 86.0%. The inverted core–shell (PS-core, PMMA-shell) morphology is seen in (a) and (b).

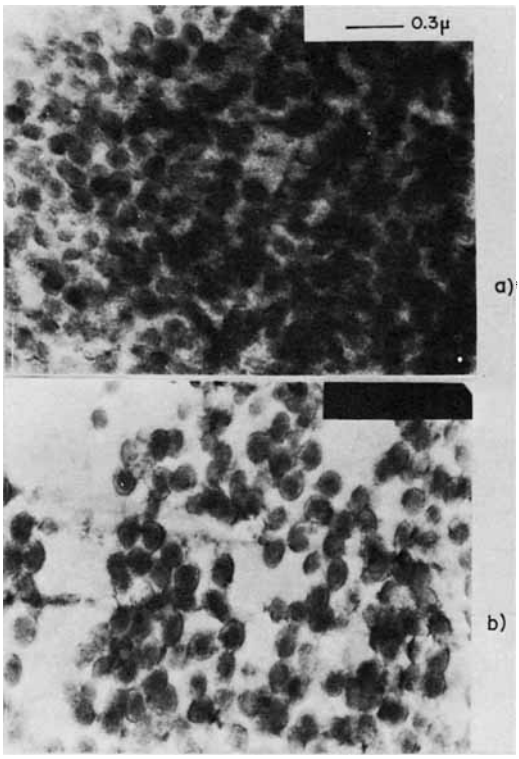

Fig. 7. Change of internal morphology of PMS-54 during the polymerization ($K_2S_2O_8$ concentration, 0.003 g/dL). The monomer conversions were (a) 22.1% and (b) 47.8%. The inverted core–shell morphology can be deduced.

after call this morphology "sandwichlike." In the case of PMS-30 the PS-rich domain started in the similar way as PMS-31, as shown in Figure 9. However, in this case the PS-rich domains gradually covered the PMMA-rich region. And finally the "core–shell" morphology emerged. This core–shell morphology was also observed in PMS-24 (Fig. 10) and PMS-52 (TEMs are not given) with a little difference. In the cases of PMS-5, -6, and -19,

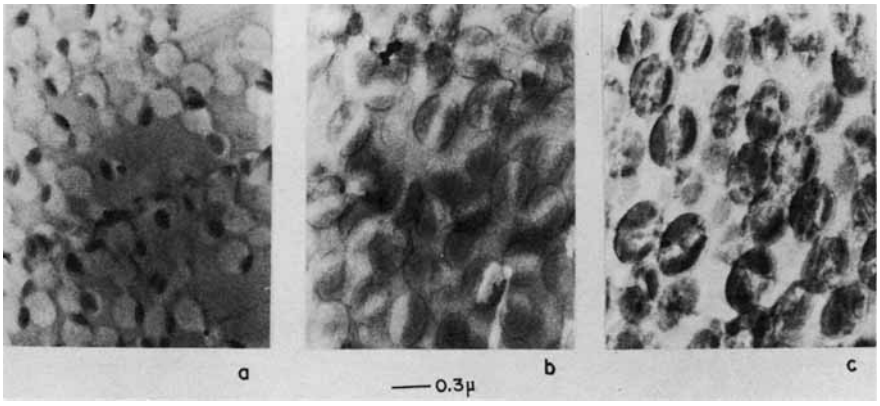

Fig. 8. TEMs of RuO_4-stained thin sections. Change of internal particle morphology of PMS-31 during the polymerization at 60°C. The monomer conversions were (a) 3.7%, (b) 31.4%, and (c) 92.5%. The dark PS-rich regions sandwiched the bright PMMA region as shown in (b).

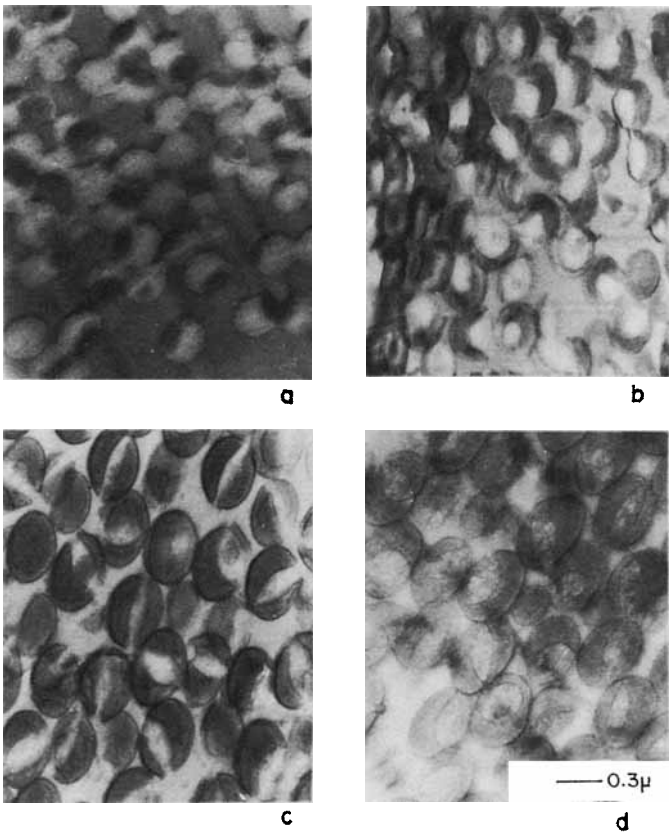

Fig. 9. TEMs of RuO_4-stained thin sections. Change of internal particle morphology of PMS-30 during the polymerization at 80°C. The monomer conversions are (a) 6.1%, (b) 43.9%, (c) 57.5%, and (d) 99.4%. The core–shell (PS-shell, PMMA-core) morphology is seen in (b) and (c).

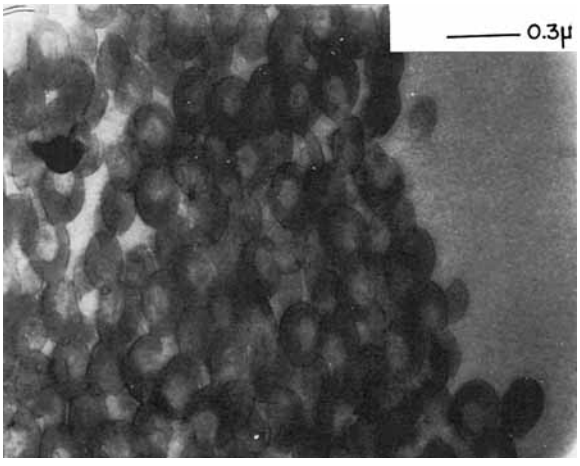

Fig. 10. TEMs of RuO_4-stained thin section of PMS-24 (polymerization temperature, 80°C). The core–shell morphology (PS-shell, PMMA-core) can be identified.

the PS-rich domain grew only at one side of a particle, and we called the resulting morphology "halfmoonlike" (cf. Fig. 1). The latex particles in PMS-31 or PMS-5, -6, and -19 grew into either the sandwichlike or halfmoonlike shape in somewhat mixed modes. However, the major morphology of the particles were distinct enough to classify them either as sandwichlike or as halfmoonlike.

Interfacial tension[9] could also play important roles in determining the morphology of monomer-swollen particles, when they were dispersed in water. Those relevant interfacial tension values were shown in Table V. Those of PS and PS(emulsion polymerized)–styrene to water were greater than those of PMMA and PMMA(emulsion polymerized)–styrene. However, the interfacial tension of PS(emulsion polymerized)–styrene was far lower than that of PS(bulk polymerized)–styrene. It indicated that the difference between interfacial tension of PS–styrene and PMMA–styrene might not be observable in the presence of emulsifier or the polymer with ionic terminal groups.

The rate of decomposition of $K_2S_2O_8$ was temperature-dependent, and the concentration of $—SO_4^-$ group incorporated into the particles could be different under different polymerization conditions. As shown in Figure 11, the polymerizations were virtually completed by peak time. If all the sulfate anion radicals had been produced before peak time and successfully initiated the styrene polymerization in the seed particles, the amounts of sulfate groups coupled with PS molecules could be estimated, and the results are summarized in Table VI.

As shown in Table VI, the particle morphology changed from an inverted core–shell (PS-core, PMMA-shell) to a core–shell with the increase in the concentration of the $—SO_4^-$ group coupled with PS. From these results it could be stated that the anchoring effect exhibited by terminal $—SO_4^-$ group could lead to exhibited important consequence upon the control of particle morphology. Matsumoto and his co-workers[6] concluded in their work on the poly(ethyl acrylate) (PEA)–PS system that the morphology was influenced not by an anchoring effect but by the viscosity of reaction loci. However, in those systems the ratios of PEA–PS were either below or equal to 1.0 so that during the polymerization the viscosity of the polymerization loci was greater than that of PMMA–PS and could affect to a greater degree the morphology of the particle. Lee and Ishikawa[14] also studied the inverted

TABLE V
Interfacial Tension Values of Styrene, Polymer, and Polymer Solutions to Water at 20°C

Polymer solution	Interfacial tension (dyn/cm)
Styrene	40–43[a]
PS	32.7[a]
PS + styrene[b]	33.2
PS + styrene[c]	22.3
PMMA	26.0
PMMA + styrene[d]	20.5

[a] The values were cited from Ref. 25.

[b] Bulk polymerized PS was used (concn, 1.0 wt %).

[c] Emulsion polymerized PS was used (concn, 1.0 wt %). From the reprecipitated PS, emulsifier was extracted with methanol in Soxhlet extractor for 4 days.

[d] Emulsion-polymerized PMMA was used (concn, 1.0 wt %).

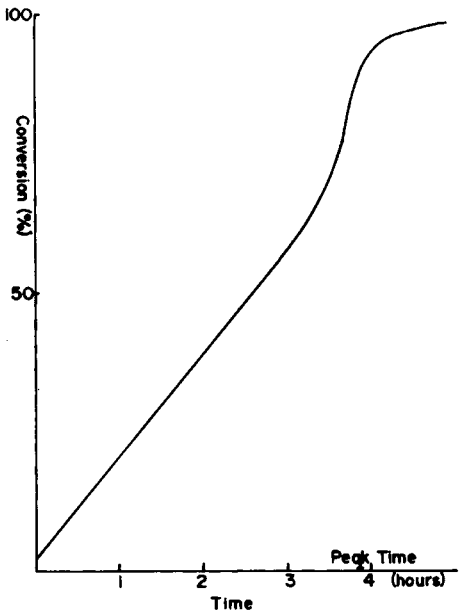

Fig. 11. Relationship between conversion and time. At the peak time the polymerization (ca. 92%) was virtually complete.

core–shell morphology, but in their systems the functionality of monomeric —COOH was too excessive to be affected by the terminal functional groups introduced by ionic initiators.

In all the PMMA-seeded polymerizations of styrene, PS– and PMMA–styrene phases normally separated clearly before the autoacceleration stage took place. Along with the polymerization the morphology of particles went through transformations to the various types. In this transformation process the mobility of polymer molecules were restricted due to the high viscosity of polymerization loci. The polymerization and the volume contraction in the PS-rich region proceeded uniformly, but in the PMMA-rich region the polymerizing PS molecules could not migrate into the PS-rich region, resulting in the formation of isolated small PS-rich domains in the PMMA-

TABLE VI
Amounts of $-SO_4^-$ Groups Coupled with PS Molecules per Unit Weight of PS[a]

Experimental no.	Peak time (min)	Polymerization temp (°C)	$W_{SO_4^-}$[b] ($\times 10^4$ g/g)	Morphology
PMS-54	306	80	1.14	Inverted core-shell
-19	230	60	2.04	Halfmoonlike
-31	588	60	4.97	Sandwichlike
-52	480	60	16.5	Core–shell
-24	97	80	19.6	Core–shell
-30	135	80	24.8	Core–shell
-40	31	80	22.3	Raspberrylike

[a] The decomposition rate constants of $K_2S_2O_8$ were 3.16×10^{-6} and 9.16×10^{-5} s^{-1} at 60°C and 80°C, respectively (cf. Ref. 26).

[b] Weight of $-SO_4^-$ coupled with unit weight of PS.

rich region, and volume contraction in the PMMA-rich region could not take place in an orderly manner. Thus, the PMMA-rich region of the completely polymerized particles became mixed with small PS domains [Figs. 6(c), 8(c), 9(d), and 10] forming various anomalous particle shapes [Figs. 1(a), 1(b), 3(d), 4(d), 5(c), 12(b), and 12(c)].

In the cases of PMS-24, -30, and -53 the formation of the void-containing particles in small conversion level were confirmed by TEMs [Fig. 4(b)] and SEMs [Fig. 12(a)]. These morphologies have been reported in soap-free styrene emulsion polymerizations,[28] PMMA–PS[10] and PBA–PS[11] composite latexes. According to Cox and co-workers,[28] the voids in PS particles were formed by the vaporization of monomer from the swollen particles during the sample preparation for TEMs. The swollen particles were composed of monomer-rich cores and polymer-rich shells. In the formation mechanism of PBA–PS void particles,[11] the PBA-rich region was effused out from the PBA-core/PS-shell composite particles in the process of the specimen preparation for electron microscopy because of the low glass transition temperature (−54°C) of PBA. However, the formation mechanism of PMMA–PS particles such as that are described above were not suggested.[10]

A schematic representation of styrene-free core–shell, halfmoonlike, sandwichlike, and inverted core–shell type particles, and the corresponding particles swollen by styrene, were shown in Figure 13. The shapes of swollen particles in a latex state are assumed from the premises that they must maintain the phase-separated sphere morphology because of the surface tension and their limited solubility in monomer. These sphere particles became the void-containing or other shapes according to their initial swollen state, being caused by initiator anchoring effects. It is obvious that the volume contraction of PMMA-rich region is much larger than that of PS-rich region during the specimen preparation for electron microscope, consequently generating the various morphologies as illustrated in Figure 13.

Effects of Viscosity

In the previous section the anomalous particle morphology at the final stage of polymerization was discussed. Since these phenomena were as-

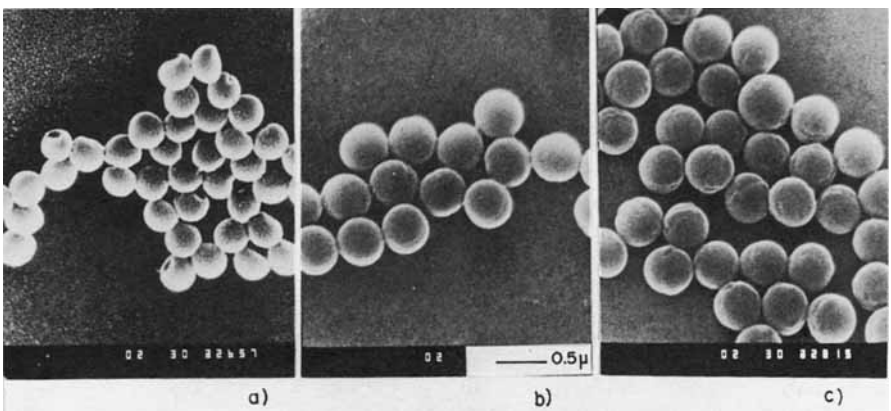

Fig. 12. SEMs of PMS latexes. Three-dimensional shapes of (a) PMS-30-4 (monomer conversion, 26.9%), (b) PMS-30 (99.4%) and (c) PMS-31 (92.5%) are shown. The void-containing (a), the core–shell (b), and the sandwichlike (c) morphologies can be deduced.

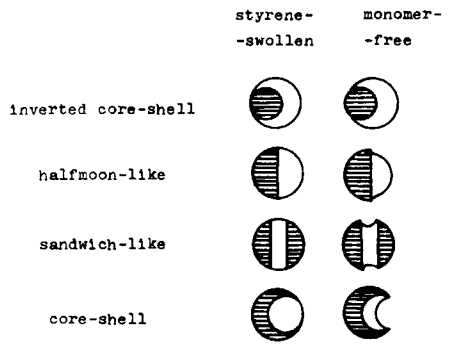

Fig. 13. Schematic representation of various morphologies of styrene-swollen and monomer-free state particles: (○) PMMA-rich region; (◍) PS-rich region.

sumed to be caused in part by the high viscosity of polymerization loci, the effects of viscosity on the particle morphology were examined.

Effects of High Viscosity. In the semibatch or the batch (swelling ratio $\leq$ 1.0) seeded emulsion polymerizations, the polymerization loci could be kept highly viscous (Table VII). The particle morphology of PMMA-seeded emulsion polymerization in highly viscous systems (semibatch and batch) was studied by soap titration methods by Okubo and his co-workers.[9] According to their work, the morphology of the latex particles obtained in semibatch polymerization changed from the initial surface localization of PS to polymeric oil-in-oil (POO) dispersion of PS in PMMA matrix and then to raspberrylike types. Above 60% of total PS content the particles finally became spherical again. In batch polymerizations the morphology of composite particles changed in the similar way to that of semibatch polymerization except the initial stage in which the surface localization of PS on a PMMA particle took place. According to these authors, PS molecules formed on the surface of PMMA particles were crushed into the interior of a particle (POO dispersion stage) by more hydrophilic PMMA to form the raspberrylike particles.

During the semibatch polymerization of PMS-45 the apparent particle shape changed from the spherical, the raspberrylike to the irregular shapes.

TABLE VII
Polymerizations under High Viscosity Conditions

Experimental no.	PMS-36	PMS-37	PMS-40	PMS-45	PMS-51
Ingredients[a]					
Water	95	95	95	95	95
PMMA (species)	5 (-5)	5 (-5)	5 (-4)	5 (-6)	5 (-7)
Styrene	15	15	5	15	5
$K_2S_2O_8$	0.1	0.1	0.1	0.1	0.1
KOH (0.1*N*)	5	5	5	5	5
Polymerization method	Semibatch	Semibatch	Batch	Semibatch	Batch
Dropping rate (mL/min)	0.6	0.6	—	0.6	—
Polymerization temp (°C)	80	60	80	60	80

[a] Quantities are in weight parts.

And the monodispersed particle size of seed latex particles became gradually broadened as PS content increased. These nonuniform shapes appeared regardless of the polymerization temperature [Figs. 14(a), 14(b)]. We attributed this phenomenon to the fact that the monomer distribution throughout the particles was not uniform because of the insufficient mixing caused by the high viscosity and the monomer in the monomer-starved particles was polymerized rapidly by Tromsdorff effect. The particle morphology was certainly affected by high viscosity as pointed out by Okubo and his co-workers.[9] However, we found that the anchoring effect of $-SO_4^-$ groups contributed significantly to the localization of PS-rich domains at the surface area of the particles. And as shown in Figure 14(c), the PMMA-rich region was surrounded by post-polymerized PS (PS/PMMA = 3). The smooth surfaces of PS-rich region in Figures 14(a) and 14(b) were formed by the increased PS volume spreading locally over the particle.

The changes in particle morphology taking place in the batch polymerization (styrene/PMMA = 1) are shown in Figure 15. At the initial stage of polymerization (Fig. 15(a); conversion, 5.5%), the PS phase was not distinguishable. But at the level of 28% conversion the PS-rich domains were identifiable at the surface region of particles, even though the contrast was not clear. Toward the end of polymerization the clear PS-rich domains surrounded almost all the surface of PMMA-rich region. Although in these polymerizations the monomer concentration in the particle was greater than in semibatch polymerizations, the mobility of polymer molecules were also limited by the high viscosity. Accordingly, the mobility of the PS-rich region was restricted, and PS domains were formed at the surface area of particles.

Effects of Low Viscosity. The viscosity of polymerization loci could be lowered by the control of polymer molecular weight or by the addition of an inert solvent (Table VIII).

When the particle morphology of PMS-32 (Fig. 16) was compared with that of PMS-31 [Fig. 8(c)], PS-rich domains in PMMA-rich phase were re-

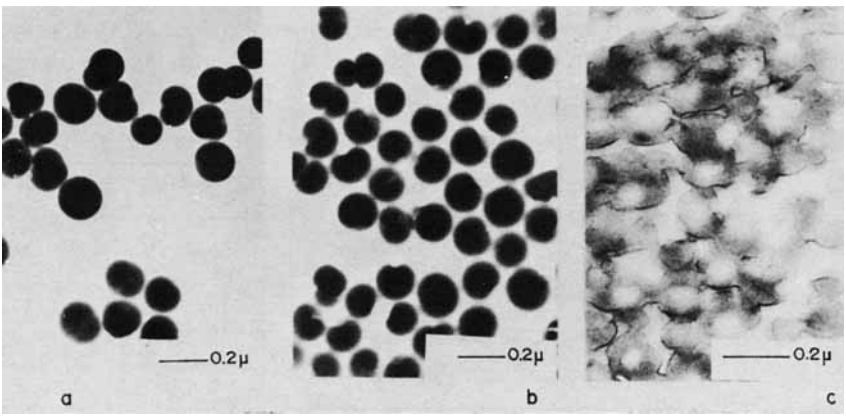

Fig. 14. Latex TEMs (a,b) and TEM of RuO_4-stained thin section (c). (a) PMS-36 [polymerization temp, 80°C]; (b,c) PMS-37 [polymerization temp, 60°C; (b), (c)] gave almost the same morphologies. In (c) the PMMA-rich region was surrounded by PS-rich region (core–shell morphology).

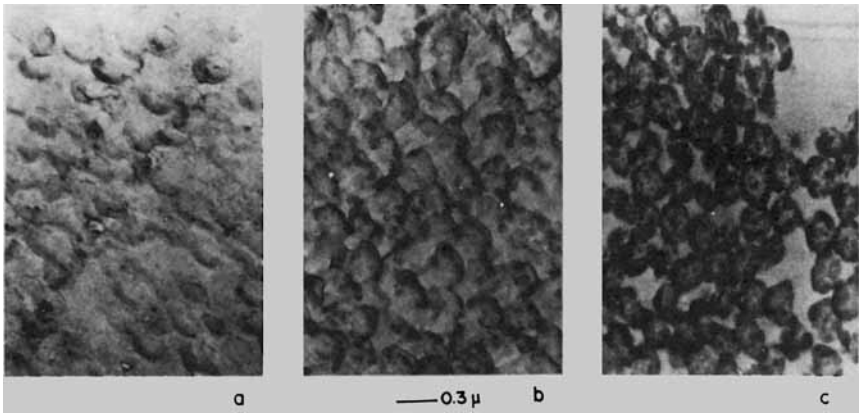

Fig. 15. TEMs of RuO_4-stained thin sections. Change of internal particle morphology of PMS-51 at 80°C (styrene/PMMA = 1.0) The monomer conversions were (a) 5.5%, (b) 27.0% and (c) 99.2%. The dark PS domains gradually covered and were clearly identifiable over the particle surface.

duced, and the easier phase separation of the PS-rich region from the PMMA-rich region was observed. The interparticle coalescence of PS-rich phases was also observed in the former case (PMS-32). These results could be attributed to the better mobility of PS molecules of low molecular weight.

Swelling of the polymerizing particles with inert solvents was chosen by many authors for kinetic studies[29] and for particle size enlargement.[30] For the purpose of decreasing the viscosity in polymerization loci, toluene was added into the polymerization systems PMS-41 and -42. The rate of polymerization decreased, and the autoacceleration stages were not observed. These results were based on the viscosity reduction of the polymerization loci by dilution of the system with toluene. Consequently, polymer molecules became more mobile and facilitated the phase separation of PS-rich and PMMA-rich phases, and the low concentration of PS in PMMA-rich regions provided the smooth particle surface (Fig. 17).

The high viscosity at the autoacceleration stages restricted the long-range movements of polymer molecules, thus making the merge of PS-rich domains in the PMMA-rich region difficult. This restricted mobility of polymer molecules could be relieved by the addition of cosolvent, and the particle

TABLE VIII
Polymerization under Low Viscosity Conditions[a]

	PMS-32	PMS-41	PMS-42
Ingredients			
Water	95	95	95
PMMA (seed)	5 (PMMA-4)	5 (-5)	5 (-5)
Styrene	15	15	15
KOH (0.1*N*)	5	5	5
$K_2S_2O_8$	0.1	0.1	0.1
Toluene		5	5
$CHBr_3$	0.1		
Conditions			
Polymerization temp (°C)	60	80	60

[a] Quantities are in weight parts.

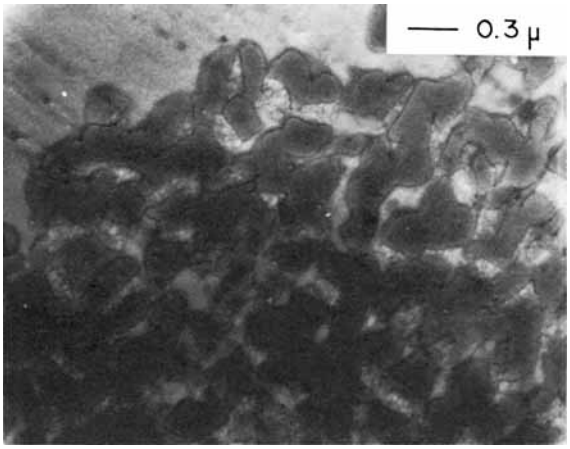

Fig. 16. TEM of RuO_4-stained thin section of PMS-32 at 60°C. Because of the low molecular weight of PS, when polymerized with $CHBr_3$, the phase separation between PS-rich region and PMMA-rich domains and the interparticle coalescence occurred easily.

morphology was transformed to the thermodynamically stable form. The representative morphology of thus obtained particles is shown in Figure 18. The raspberry PMS-40 particles were transformed to the halfmoonlike type by the merge of PS domains.

According to the calculated value $W_{SO_4^-}$ (cf. Table VI) the equilibrium swelling morphology of PMS-40 should be the core–shell type, but it was the halfmoonlike. Because of the high viscosity of polymerization loci, the polymerization was autoaccelerated, and almost all the monomer was polymerized not by incoming initiator radicals but by unterminated radicals. Therefore, the fraction of sulfate anion radicals which were coupled with PS exhibiting anchoring effect was smaller than the total decomposed sulfate anion radicals, and the halfmoonlike morphology was formed.

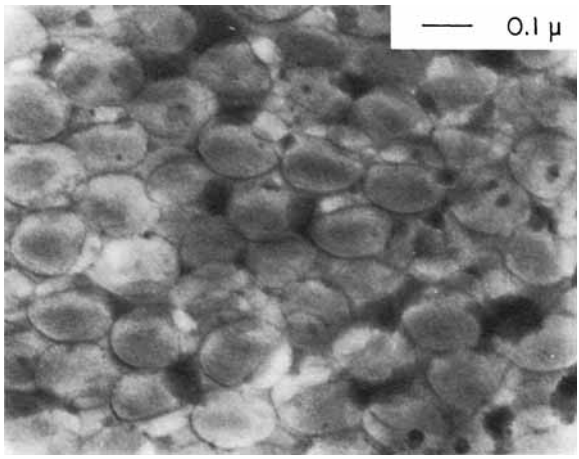

Fig. 17. TEM of RuO_4-stained thin section of PMS-42 at 60°C. Because of low viscosity in the toluene-swollen particle the phase separation between PS-rich and PMMA-rich regions occurred clearly.

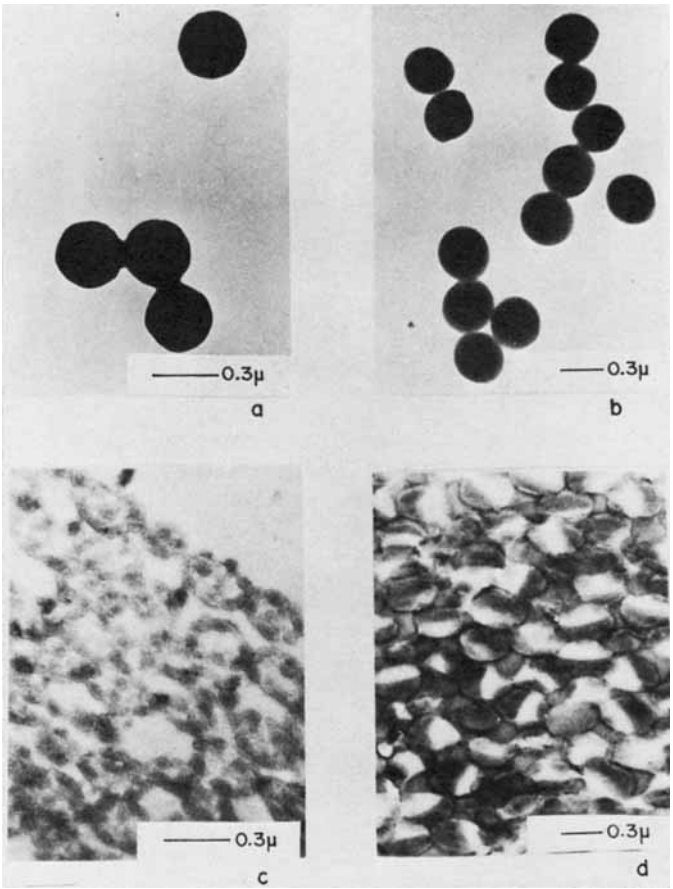

Fig. 18. Latex TEMs (a,b) and TEMs of RuO_4-stained thin sections (c,d) of PMS-40. Before benzene swelling the particles were shown raspberry morphology (a,c). But after benzene swelling the particle morphology was changed to the halfmoonlike morphology (b,d).

CONCLUSION

The morphology of composite latex particles prepared by PMMA-seeded emulsion polymerization of styrene could be controlled by various polymerization reaction parameters. In batch polymerizations, the equilibrium swelling at each polymerization temperature could be attained during the warmup time (about 1 h). Thus the long swelling time at room temperature before polymerization did not affect the particle morphology. The decomposition rate of $K_2S_2O_8$ remained unchanged in the pH range 3–12, and in this pH range the particle morphology was not affected. The anchoring effect exhibited by the terminal functional groups originated from the ionic initiators affected significantly the particle morphology. Oil-soluble hydrophobic initiator AIBN and water-soluble but less hydrophilic initiator ABCVA gave inverted core–shell morphology. When water-soluble hydrophilic initiator $K_2S_2O_8$ was employed, the particle morphology changed from the inverted core–shell, the halfmoonlike, the sandwichlike to the core–shell type. These morphological variations were dictated by the amount of the bounded $—SO_4^-$ on PS phase, and the latter was controlled by the

TABLE IX
Morphology Change of PMMA–PS Composite Particles Observed under Various Polymerization Conditions.

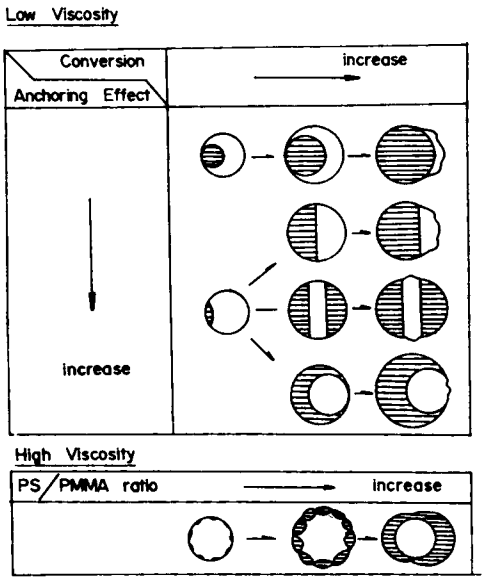

[a] (◯) PMMA-rich region; (◍) PS-rich region.

initiator concentration and the polymerization temperature. Viscosity of polymerization loci controlled the mobility of polymer molecules. Therefore, the high viscosity of polymerization loci gave the uneven morphology of particles in which the PS-rich domains were present in the PMMA-rich region. However, at low viscosity the smooth particle and the clear phase separation between the PS-rich and PMMA-rich regions resulted. In the semibatch polymerizations the monodispersity in particle size were not obtained when monomer conversion increased, and, at PS/PMMA = 3.0, the PS shelled the PMMA-core.

A schematic representation of different morphological transformations we have observed in the present investigation is summarized in the Table IX.

We are indebted to Mr. C. M. Oh, Mr. S. A. Song, and Miss I. S. Han of Lucky Central Research Institute for the electron microscopy works.

References

1. E. Schmidt, U. S. Pat. 3,673,133 (1972).
2. W. V. Smith, *J. Am. Chem. Soc.*, **70**, 3695 (1948).
3. L. J. Hughes and G. L. Brown, *J. Appl. Polym. Sci.*, **5**, 580 (1961).
4. T. R. Paxton, *J. Colloid Interface Sci.*, **31**, 19 (1969).
5. R. A. Dickie, M.-F. Cheung, and S. Newman, *J. Appl. Polym. Sci.*, **17**, 65 (1973).
6. T. Matsumoto, M. Okubo, and S. Shibao, *Kobunshi Ronbunshu*, **33**, 575 (1976).
7. M. Okubo, Y. Katsuta, A. Yamada, and T. Matsumoto, *Kobunshi Ronbunshu*, **36**, 459 (1979).
8. M. Okubo, Y. Katsuta, and T. Matsumoto, *J. Polym. Sci., Polym. Lett. Ed.*, **18**, 481 (1980).
9. M. Okubo, A. Yamada, and T. Matsumoto, *J. Polym. Sci., Polym. Chem. Ed.*, **16**, 3219

(1981).

10. M. Okubo, M. Ando, A. Yamada, Y. Katsuta, and T. Matsumoto, *J. Polym. Sci., Polym. Lett. Ed.*, **19**, 143 (1981).

11. M. Okubo, Y. Katsuta, and T. Matsumoto, *J. Polym. Sci., Polym. Lett. Ed.*, **20**, 45 (1982).

12. D. I. Lee, *Am. Chem. Soc., Div. Org. Coat. Plast. Chem., Pap.*, **43**, 622 (1980).

13. D. I. Lee, Preprints of the 2nd Japan-Korea Joint Symposium on Polymer Science and Technology, Kyoto, 1980, p. 37.

14. D. J. Lee and T. Ishikawa, *J. Polym. Sci., Polym. Chem. Ed.*, **21**, 147 (1983).

15. T. I. Min, A. Klein, M. S. El-Aasser, and J. W. Vanderhoff, *J. Polym. Sci., Polym. Chem. Ed.*, **21**, 2845 (1983).

16. K. Kato, Jpn. Plast., **2**(Apr.), 6 (1968).

17. (a) J. S. Trent, J. I. Scheinbeim, and P. R. Couchman, *J. Polym. Sci., Polym. Lett. Ed.*, **19**, 315 (1981); (b) J. S. Trent, J. I. Scheinbeim, and P. R. Couchman, *Macromolecules*, **16**, 589 (1983).

18. L. H. Sperling, T.-W. Chiu, and D. A. Thomas, *J. Appl. Polym. Sci.*, **17**, 2443 (1973).

19. W. V. Smith and R. H. Ewart, *J. Chem. Phys.*, **16**, 592 (1948).

20. M. Morton, S. Kaizerman, and M. W. Altier, *J. Colloid Sci.*, **9**, 300 (1954).

21. Y. Chung-Li, J. W. Goodwin, and R. H. Ottewill, *Progr. Coll. Polym. Sci.*, **60**, 163 (1976).

22. S. M. Hasan, *J. Polym. Sci., Polym. Chem.* **20**, 3031 (1982).

23. D. C. Blackley, *Emulsion Polymerization*, Applied Science, London, 1975, pp. 155–250.

24. R. J. Kern, *J. Polym. Sci.*, **21**, 19 (1956).

25. B. R. Vijayendran, *Polymer Collids II*, R. M. Fitch, Ed., Plenum, New York, 1980, pp. 71–83.

26. *Polymer Handbook*, J. Brandrup and E. H. Immergut, Eds., Wiley, New York, 1975, p. II-40.

27. G. E. Molau: (a) *J. Polym. Sci. Part A*, **3**, 1267 (1965); (b) **3**, 4235 (1965).

28. R. A. Cox, M. C. Wilkinson, J. M. Creasey, A. R. Goodall, and J. Hearn, *J. Polym. Sci., Polym. Chem. Ed.*, **15**, 2311 (1977).

29. D. C. Blackley and A. Haynes, *Br. Polym. J.*, **9**, 321 (1977).

30. J. Ugelstad and P. C. Mork, *Adv. Colloid Interface Sci.*, **13**, 101 (1980).

Received June 29, 1984
Accepted August 30, 1984